

In Vivo MRI and Intravital Optical Microscopy of Window Chambers in Mice

A. F. Gmitro^{1,2}, S. Moore³, R. Gatenby¹

¹Department of Radiology, University of Arizona, Tucson, AZ, United States, ²College of Optical Sciences, University of Arizona, Tucson, AZ, United States,

³Biomedical Engineering, University of Arizona, Tucson, AZ, United States

Introduction: MRI of mouse models is a powerful method of investigation in cancer biology. It is used routinely to study anatomic, physiologic, and functional aspects of tumor growth and tumor microenvironments [1]. Intravital optical microscopic imaging of implanted window chambers in mouse models is another approach for studying tumor microenvironments. It provides a method for direct high resolution imaging of tumors and the tumor-host interface. Optical imaging of window chambers can be used to study the vascular, pH, and oxygen distributions within tumors and surrounding normal tissues [2]. A key issue in both MRI and optical studies of biological properties is validation of methods. Although relative changes can be appreciated it is often difficult to assess the absolute accuracy of quantitative measures of many of the relevant biological parameters. Cross validation of one technique (e.g. MRI) by another (e.g. intravital microscopy) could provide such an assessment. Here we report on the first in vivo experiments to demonstrate the dual imaging modalities of MRI and intravital optical microscopy.

Methods: Window chambers consisting of front and back planar pieces were made of Plexiglas to mimic the basic geometry of conventional metal window chambers. To mount a window chamber (wc), the dorsal skin flap of the mouse is pulled up and sewn to the top of the back chamber piece. The outer layer of skin within the 1 cm window region is removed and then the top piece with the hole for the window is screwed down with plastic screws onto the back piece. A circular glass coverslip is placed over the exposed tissue and held in place with a clip ring. Tumor cells (PC3N/eGFP) were implanted under the coverslip and allowed to grow for approximately 1 week. Optical imaging of wc was performed with a Nikon E600/C1 confocal microscope. Magnification could be varied to image the whole window at low resolution (1X objective, 1.2 cm FOV, 25 $\mu\text{m}/\text{pixel}$) or selected fields within the chamber at higher resolution (e.g. 20X objective, 0.6 mm FOV, 0.6 $\mu\text{m}/\text{pixel}$). Optical imaging of the GFP expressing tumor cells was done via Ar laser excitation at 488 nm and fluorescence emission at 515/30 nm. Imaging of pH distribution was accomplished using tail vein injection of SNARF, an exogenous fluorescent dye whose spectral emission characteristics are dependent on local pH, excitation with HeNe laser at 543 nm, and dual collection of fluorescence emission at 595/50 nm and 640 nm lp. The ratio of signal intensity in the two emission bands I640/I595 increases monotonically with pH. Calibration data were used to convert ratio values to pH. MRI was done on a 4.7 T Bruker Biospec using a volume coil for excitation and 1 inch surface coil receiver mounted above (parallel to) the wc. The metal clip ring was removed before MR imaging. A holder was used to place the mouse on its side with the wc horizontal in the magnet. T1-weighted spin echo imaging was performed in the coronal (perpendicular to wc) and sagittal (parallel to wc) planes. Sequence parameters were: TR=500ms, TE=15ms, matrix=256x256, FOV=2.56x256cm, and NEX=8 (scan time 17min). For coronal imaging 12 1mm slices covered the wc. For sagittal imaging a 4 mm slice was sufficient to capture the wc in a single image. After pre-contrast imaging, 0.2 ml gadolinium-based contrast (Magnevist; Berlex Laboratory, Wayne, NJ, USA) diluted 5:1 with normal saline was injected via tail vein catheter. Sagittal and coronal MRI was repeated.

Results: Fig. 1 shows MR images of the window chamber, coronal image in Fig 1a, pre-contrast sagittal image in Fig 1b, and post-contrast sagittal image in Fig. 1c. The sutures holding the tissue in place are seen in the upper right corner of the sagittal images. Fig. 2 shows a series of images from the same animal over a subregion of the wc where the tumor is located. Fig 2a is the difference between Figs. 1b and 1c, which shows the tumor region with increased contrast uptake. Fig. 2b is the optical fluorescence image of the GFP showing where the tumor cells are located. Fig. 2c is an optical transmission image showing where the blood vessels are located, and Fig. 2d is a pH image. In this case the tumor has lower pH, which corresponds to the darker signal intensity.

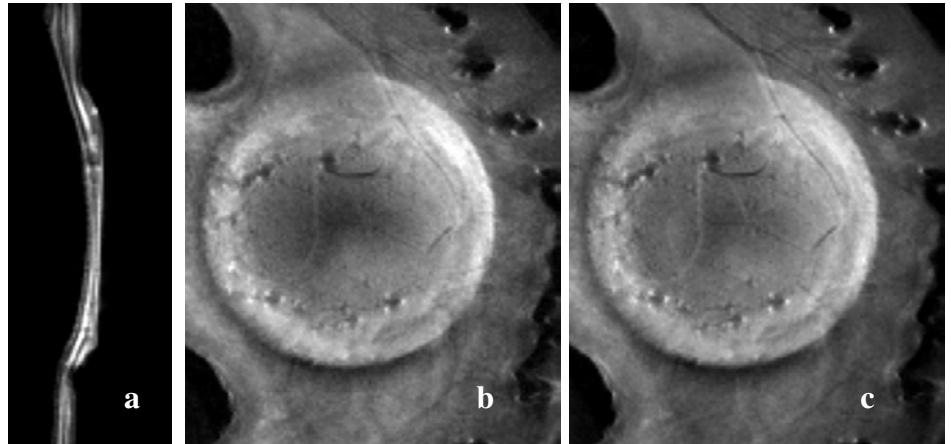


Fig. 1 MR images of window chamber, a) coronal image, b) pre-contrast sagittal image, c) post-contrast sagittal image.

Discussion: The results of Figs 1 and show that high resolution MR and optical imaging of window chambers implanted in a mouse model can be achieved in vivo. This methodology allows correlative studies to be done to independently assess and validate the measurement accuracy of many important tissue properties, such as pH, tumor oxygenation, perfusion, vascular distribution and vascular permeability.

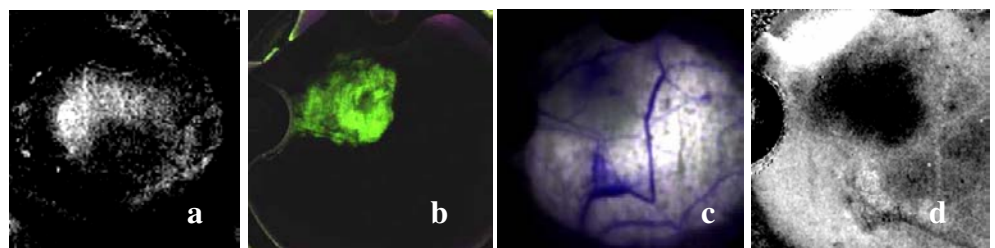


Fig. 2 Window chamber images, a) MR difference image, b) GFP intravital microscopy image, c) Optical transmission image, and d) pH image calculated from ratio of SNARF fluorescence images.

Acknowledgement: This work is supported by NIH (CA093650).

References: [1] Gillies RJ, J Magn Reson Imaging, 16:430, 2002. [2] Dewhirst M, Dis Markers 18:293 2002.